micro

MDPI

Article

Synthesis, Characterization, and Antibacterial Activity of Silver Nanoparticle-Based Biopolymer Formulations Against *Escherichia coli* for Food-Related Applications

Anuarbek Suychinov [1], Kamil Derbyshev [2], Zhanibek Yessimbekov [1], Dastan Asserzhanov [2] and Eleonora Okuskhanova [2,*]

[1] Kazakh Research Institute of Processing and Food Industry (Semey Branch), 29 Baitursynov Street, Semey 071410, Kazakhstan; asuychinov@gmail.com (A.S.); zyessimbekov@gmail.com (Z.Y.)
[2] Research School of Food Engineering, Shakarim University, 20A Glinki Street, Semey 071412, Kazakhstan; derbyshev_kamil@mail.ru (K.D.); dastan2194.as@gmail.com (D.A.)
* Correspondence: eokuskhanova@gmail.com

Abstract

Foodborne microbial contamination remains a major challenge for the safety and shelf life of poultry and other perishable foods. This study developed a silver nanoparticle (AgNP)-based antimicrobial formulation and evaluated its physicochemical characteristics, antibacterial activity against *Escherichia coli*, and preliminary concentration-dependent effects on bovine sperm viability. AgNPs were synthesized using a modified glucose–citrate reduction method. UV–Vis measurements showed characteristic surface plasmon resonance maxima within approximately 411–422 nm across the evaluated synthesis experiments. Transmission electron microscopy revealed predominantly quasi-spherical particles with a mean diameter of 23.14 ± 8.31 nm (n = 100), a median diameter of 25.30 nm, and a size range of 5.07–34.88 nm. The mean hydrodynamic radius was 15.47 nm, and the zeta potential was −38.80 ± 0.63 mV, indicating pronounced electrostatic stabilization of the colloidal dispersion. In antibacterial assays, the complete AgNP–chitosan–lactic acid–collagen formulation resulted in complete absence of visible *E. coli* growth at all tested concentrations, including the lowest evaluated nominal Ag concentration of 6.5 mg/L in the prepared formulation, corresponding to approximately 3.25 µg/mL in the final antibacterial assay mixture, whereas the other tested formulation variants did not achieve complete growth suppression. In the preliminary bovine sperm assay, AgNP dispersion alone caused a concentration-dependent decline in viability, with statistically significant effects observed from 1.37 mg/L onward. These findings demonstrate that the complete multicomponent formulation provides strong antibacterial activity at relatively low nominal Ag concentrations while also highlighting the need for further toxicological and migration assessment. Future studies should validate the formulation in real food matrices and evaluate silver release, migration, and safety under relevant storage and application conditions.

Keywords: silver nanoparticles; chitosan; collagen; antimicrobial formulation; *Escherichia coli*; food preservation; sperm viability

Check for updates

Academic Editor: Aris Giannakas

Received: 23 September 2026
Revised: 30 September 2026
Accepted: 1 October 2026
Published: 4 October 2026

Copyright: © 2026 by the authors. Licensee MDPI, Basel, Switzerland. This article is an open access article distributed under the terms and conditions of the Creative Commons Attribution (CC BY) license.

1. Introduction

Microbial contamination remains a major constraint on food quality, safety, and shelf life. Spoilage microorganisms reduce sensory acceptability and storage stability, while foodborne pathogens create direct public health risks and economic losses for producers,

retailers, and consumers [1,2]. These challenges have stimulated interest in complementary antimicrobial systems that can be incorporated into food-processing, surface-treatment, packaging, and other food-contact applications [3,4]. At the same time, increasing concern regarding antimicrobial resistance among foodborne bacteria, including *Escherichia coli*, *Salmonella enterica*, and *Listeria monocytogenes*, has strengthened interest in non-antibiotic antimicrobial strategies that can complement hygiene, refrigeration, and established preservation practices [5,6].

Poultry meat represents a particularly relevant potential application area because it is highly perishable and may become contaminated during slaughter, processing, handling, and storage. Poultry-associated microorganisms of concern include *Campylobacter* spp., *Salmonella enterica*, *Listeria monocytogenes*, and *Escherichia coli*, while spoilage microbiota such as *Pseudomonas* spp., *Brochothrix thermosphacta*, and lactic acid bacteria can reduce product quality and shelf life [3,7]. Chicken meat therefore provides an important application context for the development of complementary antimicrobial systems.

Conventional preservation and sanitation approaches remain indispensable, but they may not fully prevent microbial persistence under all processing and storage conditions. In poultry-processing environments, microorganisms are exposed to cold, desiccation, heat, and chemical stresses, which can trigger adaptive responses involving stress-protein production, altered membrane function, efflux systems, and mono- or mixed-species biofilm formation [8]. Such responses are relevant because biofilms on food-contact surfaces may act as persistent contamination reservoirs. Consequently, active packaging, antimicrobial films, coatings, and other food-contact systems have been investigated as complementary hurdles rather than replacements for good manufacturing practice, cold-chain control, or regulatory hygiene requirements [9,10].

Silver nanoparticles (AgNPs) have attracted considerable attention as antimicrobial agents because their activity is multifactorial. AgNPs may interact with bacterial surfaces, disrupt cell envelopes, increase membrane permeability, generate reactive oxygen species, release Ag^+ ions, and interfere with proteins, enzymes, nucleic acids, and intracellular signaling pathways [11–14]. These concurrent mechanisms can inhibit bacterial growth and, in some systems, interfere with biofilm formation. Importantly, antibacterial performance is not determined by silver concentration alone; it is strongly influenced by particle size, morphology, surface chemistry, surface charge, aggregation state, colloidal stability, and the composition of the surrounding matrix [11,12,15].

Food-related studies have investigated AgNPs and other antimicrobial agents in active packaging, edible films, coatings, and polymer composites as a means of combining physical protection with antimicrobial functionality [10,16,17]. For example, biodegradable films based on taro starch, sodium alginate, and nisin significantly reduced microbial load and extended the refrigerated shelf life of chicken meat, demonstrating the relevance of active antimicrobial systems for poultry products [16]. In another meat-preservation study, nanosilver treatment reduced microbial load in beef samples, with the strongest short-term effect observed at the highest tested concentration [18]. These studies provide a broader application context for the present formulation but do not represent direct experimental analogues of the current study.

The synthesis route is a critical determinant of AgNP properties because reaction conditions influence nucleation, particle growth, morphology, surface characteristics, colloidal behavior, and biological activity. The present study employed a mild aqueous glucose–citrate reduction system. Previous studies and recent reviews have shown that citrate concentration, temperature, pH, precursor concentration, reaction time, and stabilizing components can substantially influence AgNP size, morphology, and stability [11,17]. The surrounding medium can also affect dispersion behavior. Park and Lee [19], for example,

reported that citrate-capped AgNPs remained dispersed in a 5% isotonic glucose solution, whereas aggregation and precipitation occurred in phosphate-buffered saline and 0.9% NaCl.

For food-related applications, antibacterial efficacy alone is insufficient. The composition of the carrier system, the concentration of silver, the potential release of Ag^+, and the concentration-dependent effects of the nanoparticle dispersion on cell viability all require consideration. AgNP cytotoxicity is concentration-dependent and can also be affected by particle size, surface chemistry, aggregation state, exposure duration, and ion release [12,20]. Therefore, preliminary in vitro sperm viability assessment can provide an initial indication of concentration-dependent effects following AgNP exposure, although such assays cannot establish toxicological safety, regulatory compliance, or suitability for direct food-contact use.

Biopolymer-based matrices are of particular interest because they may combine structural functionality with antimicrobial activity. Chitosan has intrinsic antibacterial properties and is widely used in edible films and coatings, whereas collagen can function as a biocompatible carrier suitable for food-contact applications [21,22]. In the present formulation, collagen was incorporated as a viscous biopolymer carrier intended to provide a suitable matrix for surface application, whereas lactic acid served as a food-compatible medium for chitosan solubilization and could additionally contribute to antimicrobial activity. The formulation was designed to determine whether combining these components with AgNPs could maintain antibacterial performance while progressively reducing the amount of silver in the final system.

AgNP–chitosan systems and AgNP-containing biodegradable materials have already been widely investigated. For example, Ogungbesan et al. [23] developed a chitosan–AgNP film and evaluated its antibacterial activity and cytotoxicity, whereas das Neves et al. [24] incorporated biogenic AgNPs into biodegradable polymer films and examined antibacterial performance together with silver migration into chicken meat. Accordingly, the novelty of the present study does not reside in the AgNP–chitosan association itself. Instead, the study evaluates a multicomponent formulation in which separately synthesized glucose–citrate AgNPs are combined with chitosan solubilized in lactic acid and collagen as a biopolymer matrix. The experimental design additionally compared matched component combinations and progressively reduced the nominal Ag concentration to determine whether antibacterial activity could be retained at lower silver levels.

The aim of this study was therefore to synthesize and characterize AgNPs using a modified glucose–citrate reduction method and to evaluate their incorporation into a multicomponent antimicrobial formulation containing chitosan, lactic acid, and collagen. Particular attention was given to the physicochemical characteristics of the synthesized AgNPs, the antibacterial performance of the different formulation variants against *Escherichia coli*, and the concentration-dependent effect of the AgNP dispersion on bovine sperm viability as a preliminary biological screening model.

2. Materials and Methods

2.1. Materials and Experimental Overview

Silver nitrate ($AgNO_3$; chemically pure grade, ≥99.9%; SIBPROEKT, Moscow, Russia), D-glucose (dextrose; $C_6H_{12}O_6$), and sodium citrate ($Na_3C_6H_5O_7{\cdot}5.5H_2O$; analytical grade) were used for AgNP synthesis. Food-grade collagen and chitosan were used as biopolymer components of the antimicrobial formulation. The chitosan was derived from deacetylated chitin and had a degree of deacetylation of 75–85%, an average molecular weight of 190–310 kDa, and a reported purity of ≥75% (Sigma-Aldrich Co., St. Louis, MO, USA). Lactic acid was used to prepare the chitosan-containing component of the formu-

lation. A sterile 0.9% NaCl solution was used for preparation and dilution of bacterial suspensions. Meat-peptone broth (MPB) and meat-peptone agar (MPA) were used for bacterial cultivation and antimicrobial testing. A 5% eosin solution was used for sperm viability staining.

Bidistilled water was used for preparation of aqueous solutions and AgNP dispersions. Water was produced using a GFL 2302 glass bidistillation system (GFL Gesellschaft für Labortechnik mbH, Burgwedel, Germany). According to the instrument specifications, the resulting water had an electrical conductivity of $\leq$1.6 μS/cm at 20 °C.

The study comprised three experimental stages: (i) synthesis and physicochemical characterization of AgNPs; (ii) preparation and antibacterial evaluation of AgNP-containing biopolymer formulations; and (iii) preliminary in vitro assessment of the concentration-dependent effect of the AgNP dispersion on bovine sperm viability. Detailed procedures for formulation preparation, antibacterial testing, and sperm viability assessment are provided in Sections 2.3, 2.7 and 2.8, respectively.

2.2. Synthesis of Silver Nanoparticles

Silver nanoparticles (AgNPs) were synthesized using a glucose–citrate procedure developed from a previously reported citrate-reduction protocol [25] and informed by previous reports of glucose-mediated AgNP synthesis in the presence of sodium citrate [26]. In the reference citrate procedure [25], 80 mL of 0.002 M $AgNO_3$ is combined with 16 mL of 0.0075 M sodium citrate under heated reflux/boiling conditions and magnetic stirring, followed by continued boiling for 20 min after development of the characteristic yellow color. In the present study, glucose was introduced as an additional reducing agent, a lower amount of sodium citrate was used, the citrate-containing solution volume was increased to 30 mL, and reflux/boiling was replaced by heating in a water bath at approximately 74–75 °C with periodic manual mixing. Heating was terminated after formation of an intense yellow to yellow–olive dispersion rather than continuing boiling for 20 min.

Briefly, 80 mL of the 0.002 M silver nitrate ($AgNO_3$) solution was used as the silver precursor. A glucose–citrate solution was prepared by dissolving 35 mg of sodium citrate and 5.0 g of glucose in 95 mL of bidistilled water. A 30 mL aliquot of this solution was measured using a graduated cylinder and added to the $AgNO_3$ solution, giving a final reaction volume of 110 mL.

The reaction mixture was heated in a water bath maintained at approximately 75 °C. The temperature of the reaction mixture was monitored directly using a thermometer placed in the flask. During heating, the flask was removed from the water bath approximately four to five times and gently swirled manually for four to five circular movements to ensure mixing and allow visual assessment of color development. For a 110 mL reaction volume, formation of the characteristic intense yellow to yellow–olive colloidal dispersion occurred after approximately 22 min of heating, although the exact time depended on the initial temperature of the reagents.

Heating was discontinued when the characteristic yellow–olive color was obtained. Further heating was avoided because progressive darkening toward brown and the development of turbidity were regarded as indicators of excessive particle growth or aggregation. The resulting AgNP dispersion was allowed to cool to approximately 20 °C. No post-synthesis purification, centrifugation, dialysis, or filtration was applied because the freshly prepared colloid showed no visible particulate contamination or precipitate. The dispersion was used directly for physicochemical characterization and formulation preparation or stored at 18–24 °C in the dark or under light-protected conditions for up to two months.

2.3. Preparation of AgNP-Containing Composite Formulations

The AgNP-containing composite formulations were prepared by combining AgNP dispersion, a chitosan–lactic acid solution, and a collagen solution at a volume ratio of 1:1:1 (*v*/*v*/*v*). For the standard formulation, the chitosan component was prepared as a 1% (*w*/*w*) chitosan solution in 2% lactic acid. Briefly, 1.0 g of chitosan was mixed with 2.5 g of 80% lactic acid and 96.5 mL of distilled water. The mixture was agitated on a laboratory shaker at 30 rpm for 10–20 min at room temperature until a homogeneous, transparent to slightly brownish solution was obtained.

The standard collagen component was prepared by dispersing 10 g of food-grade collagen in 90 mL of sterile distilled water to obtain a 10% (*w*/*w*) solution. The mixture was periodically agitated at room temperature until complete dissolution, which required approximately 30–35 min. The solution was then allowed to stand for approximately 30 min to remove entrapped air bubbles.

To prepare the complete composite formulation, one volume of freshly prepared AgNP dispersion was mixed with one volume of the collagen solution, followed by one volume of the chitosan–lactic acid solution. The mixture was gently agitated until homogeneous. Thus, the standard 1:1:1 formulation prepared from the 10% collagen, 1% chitosan, and 2% lactic acid stock components contained approximately 3.33% collagen, 0.33% chitosan, and 0.67% lactic acid in the prepared formulation.

For the antibacterial screening experiments, the concentrations of the individual components were systematically varied while maintaining the 1:1:1 volumetric ratio. The chitosan–lactic acid stock component was tested at chitosan:lactic acid concentrations of 1:2%, 0.5:1%, 0.25:0.5%, and 0.125:0.25% (*w*/*w*), respectively. Collagen stock solutions ranging from 5% to 30% were evaluated. The AgNP stock dispersion had a nominal silver concentration of approximately 157 mg/L, calculated from the amount of $AgNO_3$ introduced into the reaction mixture. Serial two-fold dilutions of this dispersion with sterile distilled water were used to obtain nominal Ag concentrations of approximately 79, 39, and 20 mg/L.

Nominal Ag concentrations of 157, 79, 39, and 20 mg/L in the AgNP component corresponded to approximately 52, 26, 13, and 6.5 mg/L, respectively, in the prepared 1:1:1 formulations and to approximately 26, 13, 6.5, and 3.25 μg/mL, respectively, in the final 400 μL antibacterial assay mixtures. These silver concentrations were calculated nominal values rather than analytically measured total silver concentrations.

The complete formulations were prepared under sterile conditions immediately before antimicrobial testing. Formulations containing only selected components were prepared in parallel to evaluate the contribution of the individual constituents, as described in the antibacterial-assay subsection.

2.4. UV–Vis Spectroscopic Analysis

The optical characteristics of the synthesized AgNP dispersions were evaluated by ultraviolet–visible (UV–Vis) spectroscopy using a Specord 210 Plus spectrophotometer (Analytik Jena, Thuringia, Germany). Absorption spectra were recorded over the wavelength range of 300–700 nm, with bidistilled water used as the blank. AgNP formation was assessed from the appearance of the characteristic surface plasmon resonance absorption band in the visible region. UV–Vis spectroscopy was used as a primary method for monitoring AgNP formation and the optical characteristics of the colloidal dispersions rather than as a direct method for determining particle size [27].

In addition, an early repeat AgNP synthesis prepared with 35 mg sodium citrate was evaluated using a KFK-3-01-ZOMZ manual spectrophotometer (Zagorsk Optical-Mechanical Plant, Sergiev Posad, Russia). Absorbance was measured wavelength-by-wavelength from 400 to

440 nm at 2 nm intervals to determine the position of the SPR maximum. This dataset is presented separately in Figure 1.

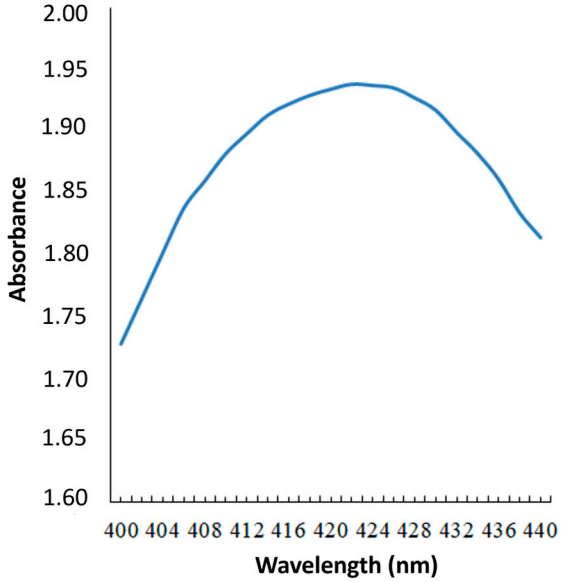


Figure 1. Absorbance profile of a AgNP dispersion obtained during an early repeat synthesis using 35 mg of sodium citrate. Measurements were performed with a KFK-3-01-ZOMZ spectrophotometer from 400 to 440 nm at 2 nm intervals; the SPR maximum was observed at approximately 422 nm.

2.5. Transmission Electron Microscopy and Particle-Size Analysis

The morphology and primary particle size of the synthesized AgNPs were examined by transmission electron microscopy (TEM) using a JEOL JEM-1400Plus microscope (JEOL Ltd., Tokyo, Japan) operated at an accelerating voltage of 120 kV. For sample preparation, a 10 µL aliquot of the AgNP dispersion was deposited onto a 200-mesh Formvar/carbon-coated copper grid and allowed to dry at room temperature before imaging.

Particle dimensions were determined from calibrated TEM micrographs using ImageJ software (version 1.54g; National Institutes of Health, Bethesda, MD, USA). A total of 100 individual nanoparticles were measured across several representative fields. Particle-size data were used to calculate the mean diameter, standard deviation, median, and observed size range, and to construct the particle-size distribution. TEM-derived measurements were interpreted as the primary particle dimensions in the dried state [28].

2.6. Dynamic Light Scattering and Zeta-Potential Measurements

The hydrodynamic characteristics and surface charge of the synthesized AgNPs were evaluated by dynamic light scattering (DLS) and electrophoretic light scattering.

The hydrodynamic radius (r_h) of the AgNPs was determined using a 3D light scattering spectrometer (LS Instruments AG, Fribourg, Switzerland). The colloidal dispersion was analyzed without additional dilution or filtration. A 0.2 mL aliquot was used for measurement and equilibrated at 25 °C before analysis. Measurements were performed at a goniometer angle of 90.06° and a temperature of 25 °C. The scattered-light intensity was approximately 30 kHz, and correlation analysis was carried out in 3D cross-correlation mode at a laser power of 0.0032 mW. The hydrodynamic radius was obtained from the translational diffusion coefficient using the Stokes–Einstein relationship [29].

Zeta potential was measured using a Litesizer 500 particle analyzer (Anton Paar GmbH, Graz, Austria) equipped with an Omega cuvette and operated using Kalliope™ software (version 2.34.3; Anton Paar GmbH, Graz, Austria). Measurements were performed at 25 °C

using automatic voltage adjustment, with a maximum applied voltage of 200 V and a Henry function value of 1.5. The AgNP dispersion was analyzed without additional dilution. Five replicate measurements were performed for zeta-potential determination [30].

2.7. Determination of Antibacterial Activity

The antibacterial activity of the AgNP-containing formulations was evaluated against *Escherichia coli* VKPM B-6645 (ATCC 25922; DSM 1103), which was obtained from the National Bioresource Center-All-Russian Collection of Industrial Microorganisms, NRC "Kurchatov Institute"—GosNIIgenetika (Moscow, Russia). Before testing, the strain was reactivated by three successive 24 h passages in meat-peptone broth and on meat-peptone agar at 37 °C.

A bacterial suspension was prepared from a 24 h culture in sterile 0.9% NaCl solution. The turbidity of the suspension was adjusted spectrophotometrically to an optical density of 0.08–0.10 at 625 nm using a KFK-3 spectrophotometer (UNICO-SYS, St. Petersburg, Russia) and a 10 mm cuvette, corresponding to an approximate bacterial concentration of 1.5×10^8 CFU/mL. The prepared suspension was used immediately for antimicrobial testing.

The antibacterial assay was developed specifically for the present study as a qualitative direct-contact screening method rather than as a standardized MIC or MBC procedure. Its design was informed by established microbiological susceptibility-testing principles and by published direct-contact approaches. For example, Talebpour et al. [31] evaluated nanoparticle-containing antimicrobial materials by placing the test preparation in direct contact with bacteria on an agar surface. In the present study, this concept was modified by mixing the bacterial suspension directly with nutrient broth and the tested formulation before application of the entire mixture to the agar surface. This approach was selected because formulation-related turbidity could interfere with broth-based optical assessment, incorporation into molten agar could expose the formulation to elevated temperatures, and diffusion-based methods could be affected by unequal diffusion of the individual formulation components.

Preliminary verification of the direct-contact procedure was performed using a commercial thermostable antimicrobial preparation. The preparation was evaluated both by the direct-contact procedure and by agar dilution using an inoculum of approximately 10^4 CFU/mL, and comparable qualitative growth-suppression outcomes were obtained. Preliminary experiments with the complete AgNP formulation also compared bacterial suspensions of approximately 1.5×10^4 and 1.5×10^8 CFU/mL; comparable qualitative outcomes were obtained, and the higher concentration was selected for the principal experiment to provide a more stringent bacterial challenge. In addition, immediate plating was compared with 2 h and 4 h pre-incubation at 37 °C in three replicate experiments. Complete suppression of visible growth was observed under all three contact-time conditions, whereas untreated controls showed bacterial growth in every replicate. Therefore, immediate plating without a separate pre-incubation period was used in the principal experiment. These preliminary experiments supported use of the procedure as a qualitative screening assay but do not constitute formal validation against a standardized antimicrobial susceptibility-testing method.

For each assay, 50 µL of the E. coli suspension (1.5×10^8 CFU/mL) was mixed with 150 µL of nutrient broth in a sterile microcentrifuge tube, followed by 200 µL of the tested formulation, giving a final volume of 400 µL and approximately 7.5×10^6 CFU per assay. The components were mixed by pipetting, and the entire 400 µL mixture was immediately applied to the agar surface without a separate pre-incubation period.

The complete formulation consisted of AgNP dispersion, chitosan dissolved in lactic acid, and collagen solution mixed at a volume ratio of 1:1:1 ($v/v/v$). Additional formulation

variants containing lactic acid alone, chitosan with lactic acid, or lactic acid combined with AgNPs and collagen were evaluated for comparison. In the complete formulations, the nominal Ag concentration in the AgNP component was varied from 157 to 20 mg/L by serial two-fold dilution of the original AgNP dispersion with sterile distilled water. These concentrations corresponded to approximately 52, 26, 13, and 6.5 mg/L nominal Ag, respectively, in the prepared 1:1:1 formulation.

The lowest tested complete formulation contained 6.5 mg/L nominal Ag in the prepared formulation, corresponding to approximately 3.25 μg/mL Ag in the final 400 μL antibacterial assay mixture.

The agar medium was meat-peptone agar in a Petri dish. The inoculum was distributed over the agar surface by gentle horizontal and circular movement of the plate. Plates were incubated at 37 °C for 20 h.

For each experimental series, the control contained 50 μL of the *E. coli* suspension, 150 μL of nutrient broth, and 200 μL of sterile distilled water instead of the antimicrobial formulation. The experiment was performed twice independently, with three Petri dishes per treatment and control in each experiment.

Separate formulation-containing blank plates without bacterial inoculation were not included in the principal experiment. During the assay, however, the agar surface was visually examined after formulation application. The formulation produced a relatively uniform cloudy area after partial drying, whereas the appearance of discrete rounded colonies identified bacterial growth. Plates without visible growth after 24 h were additionally observed for up to 3 days, and no delayed colony development was detected. Nevertheless, the absence of a dedicated formulation-only blank is considered a limitation of the visual endpoint used in this study.

Antibacterial activity was evaluated qualitatively as the presence or absence of visible bacterial growth after incubation. Visible growth was recorded as positive (+), whereas complete absence of visible growth was recorded as negative (−). The lowest tested nominal Ag concentration within the complete multicomponent formulation that resulted in complete absence of visible *E. coli* growth under the assay conditions was identified. Because no broth microdilution MIC assay, agar-diffusion assay, or confirmatory subculture from growth-negative plates was performed, the results were not interpreted as MIC, MBC, or definitive bactericidal activity.

2.8. Preliminary In Vitro Assessment of AgNP Effects on Bovine Sperm Viability

The concentration-dependent effect of the synthesized AgNP dispersion on bovine sperm viability was evaluated in vitro. Spermatozoa are sensitive to membrane damage and oxidative stress and were therefore used as a preliminary screening system for the effects of AgNP exposure [32,33]. Sperm viability after exposure was the measured endpoint. For the preliminary in vitro sperm viability assessment, AgNP dispersion alone, rather than the complete collagen–chitosan formulation, was tested using bovine spermatozoa.

Cryopreserved bovine semen in 0.24 mL straws from a Kazakh Whiteheaded bull (Krepysh/Ruslan; identification no. KZP157267) was provided by Shakarim University (Semey, Kazakhstan). The semen was diluted using a modified glucose–citrate extender prepared without ethylenediaminetetraacetic acid (EDTA) to avoid chelation of silver. The extender contained 60 g of glucose, 3.5 g of trisodium citrate dihydrate ($Na_3C_6H_5O_7 \cdot 2H_2O$), and 1.2 g of sodium bicarbonate per 1 L of distilled water.

For each sample, 0.3 mL of diluted semen was mixed with 0.2 mL of extender containing the required amount of AgNP dispersion. The final nominal Ag concentrations tested were 0.136, 0.274, 1.37, 2.74, 4.567, 6.85, 13.7, and 27.4 mg/L. A negative control

containing diluted semen and the same extender without AgNPs was prepared under identical conditions. Samples were incubated at 37 °C for 2 h before viability assessment.

Sperm viability was evaluated using an eosin dye-exclusion method based on established procedures for bovine sperm viability assessment [34]. A drop of each sample was placed on a clean glass slide and mixed with one drop of the 5% eosin solution for 1–2 s. A thin smear was then prepared and air-dried at room temperature. Spermatozoa with unstained heads were classified as viable, whereas spermatozoa with pink-to-red stained heads were classified as non-viable. Microscopic examination was performed at ×400–×600 magnification. Seven independent cryopreserved semen straws were used, and a corresponding untreated control was prepared for each semen sample, resulting in $n = 7$ independent samples for each AgNP concentration and for the control. Two slides were prepared for each concentration. A fixed number of microscopic fields was not used; instead, each smear was examined systematically by moving sequentially across adjacent fields. At least 200 spermatozoa were counted per slide, with approximately 200–500 cells evaluated in practice. Viable and non-viable spermatozoa were counted manually. Sperm viability was calculated as the percentage of unstained spermatozoa relative to the total number of spermatozoa counted. Preliminary experiments used to optimize sample handling, eosin staining, and counting procedures were excluded from the final analysis.

2.9. Statistical Analysis

Quantitative data were expressed as mean ± standard deviation (SD). Statistical analysis of the sperm-viability data was performed using Microsoft Excel 2016 (Microsoft Corp., Redmond, WA, USA). Differences among the control and AgNP exposure groups were evaluated by one-way analysis of variance (ANOVA), followed by Tukey's post hoc multiple-comparison test. Differences were considered statistically significant at $p < 0.05$.

The principal antibacterial experiment was performed twice independently, with three Petri dishes per treatment and control in each experiment. Because the antibacterial endpoint was qualitative, based on the presence (+) or complete absence (−) of visible *E. coli* growth after incubation, these results were summarized descriptively rather than subjected to parametric statistical comparison.

3. Results

3.1. Modified Glucose–Citrate Synthesis and Optical Characteristics of AgNPs

Formation of silver nanoparticles was accompanied by a progressive change in the reaction mixture from colorless to light yellow and subsequently to an intense yellow or yellow–olive color. The resulting colloidal dispersions exhibited a characteristic absorption band in the visible region attributable to the surface plasmon resonance (SPR) of AgNPs. A AgNP dispersion obtained during an early repeat synthesis with 35 mg of sodium citrate showed an SPR maximum at approximately 422 nm (Figure 1). This measurement was obtained separately using the manual KFK-3-01-ZOMZ spectrophotometer and should therefore be distinguished from the three preliminary synthesis variants subsequently compared in Figure 2.

Preliminary synthesis trials examined the effect of sodium citrate concentration and temperature control on the optical characteristics of the resulting AgNP dispersions. These three preliminary variants were separate synthesis experiments from the 35 mg sodium citrate preparation shown in Figure 1 and exhibited SPR maxima of 414.4, 420.6, and 411.3 nm, respectively. In all trials, 80 mL of 0.002 M $AgNO_3$ solution was used as the silver precursor, while the glucose–citrate component contained 5 g of glucose and the specified amount of sodium citrate dissolved in 95 mL of bidistilled water; 30 mL of this solution was subsequently combined with the $AgNO_3$ solution.

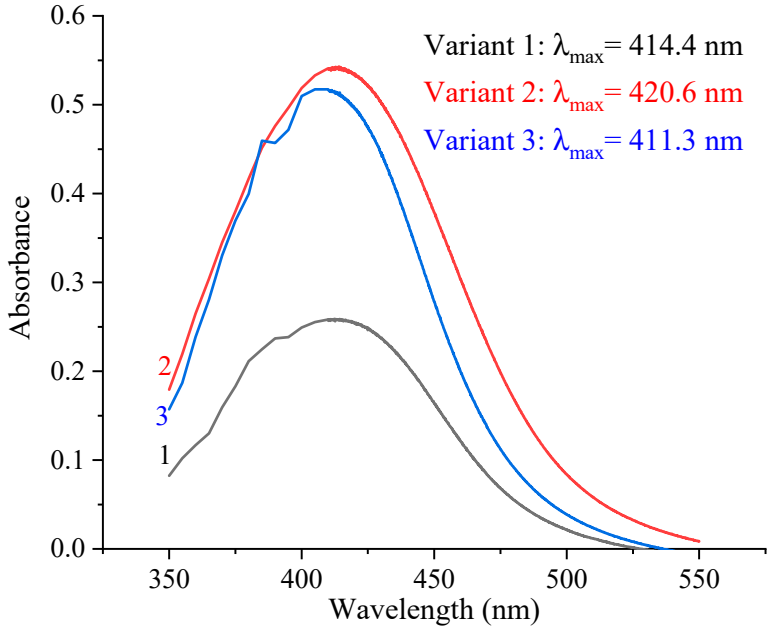


Figure 2. UV–Vis absorption spectra of AgNP dispersions obtained under different synthesis conditions: Variant 1 (black/gray curve), 70 mg sodium citrate, visual monitoring, water bath at 75 °C, λmax = 414.4 nm; Variant 2 (red curve), 70 mg sodium citrate, controlled reaction temperature of 71.5 °C, λmax = 420.6 nm; Variant 3 (blue curve), 41 mg sodium citrate, controlled reaction temperature of 72.5 °C, λmax = 411.3 nm. Variant 2 showed the highest absorbance, Variant 1 the lowest, and Variant 3 an intermediate absorbance.

In the first preliminary variant, 70 mg of sodium citrate was used and the reaction was monitored primarily by visual observation while the water bath was maintained at 75 °C. The resulting dispersion exhibited an SPR maximum at 414.4 nm and the lowest absorbance among the three compared variants (Figure 2).

In the second variant, the same amount of sodium citrate (70 mg) was used, but the temperature of the reaction mixture was monitored more closely. A light-yellow color developed after approximately 10 min, when the reaction temperature reached 70.7 °C, and an intense yellow–olive color was observed after approximately 15 min at 71.5 °C. This dispersion exhibited the highest absorbance among the compared preparations, with an SPR maximum at 420.6 nm (Figure 2).

In the third variant, the sodium citrate content was reduced to 41 mg. A light-yellow color developed after approximately 10 min at 72.3 °C, followed by more intense coloration after 15 min at 72.5 °C. The corresponding SPR maximum occurred at 411.3 nm. The corresponding SPR maximum occurred at 411.3 nm, and the maximum absorbance was intermediate between those of Variants 1 and 2. The absorption band was somewhat narrower than those observed for the 70 mg citrate preparations, indicating differences in the optical characteristics of the colloidal system (Figure 2).

The corresponding differences in the visual appearance of the three colloidal dispersions are shown in Figure 3. All preparations exhibited the characteristic yellow coloration associated with AgNP formation, although differences in color intensity were evident among the synthesis variants.

Overall, the preliminary experiments showed that changes in sodium citrate concentration and reaction-temperature control affected the position, intensity, and shape of the AgNP SPR absorption band. Across the evaluated preparations, the SPR maxima ranged from 411.3 to 420.6 nm. These observations were used to refine the synthesis procedure. For the AgNP dispersion subsequently used for physicochemical characterization and

biological experiments, the standardized synthesis protocol described in the Materials and Methods section employed 35 mg of sodium citrate.

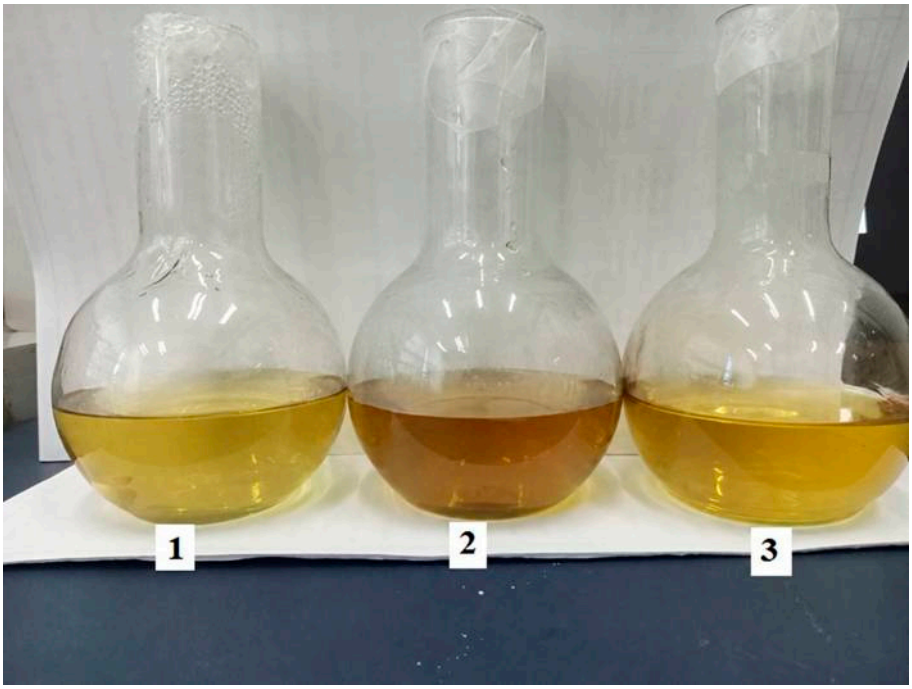


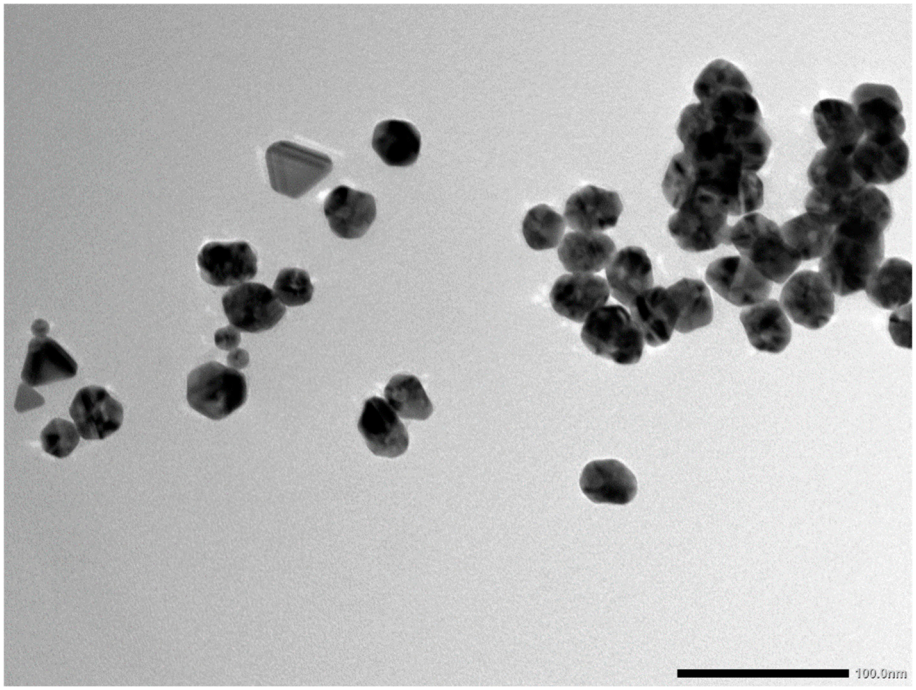
Figure 3. Visual appearance of AgNP colloidal dispersions obtained during preliminary synthesis trials: (1) 70 mg sodium citrate with visual process monitoring; (2) 70 mg sodium citrate with controlled heating to 71.5 °C; and (3) 41 mg sodium citrate with controlled heating to 72.5 °C.

3.2. Morphological Characteristics, Hydrodynamic Radius, and Zeta Potential of AgNPs

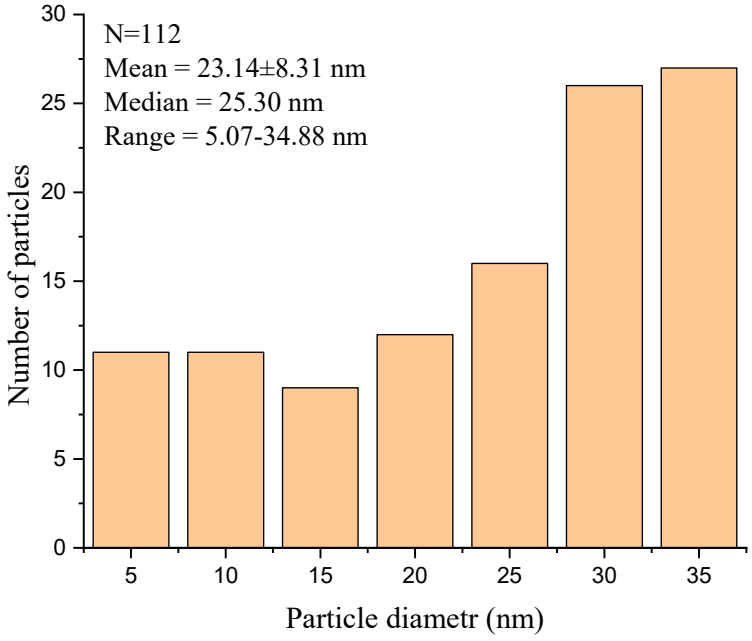
Transmission electron microscopy confirmed the formation of nanoscale AgNPs with predominantly quasi-spherical morphology, together with occasional irregular, polygonal, triangular, and other anisotropic particles (Figure 4A). Quantitative analysis of 112 individual particles yielded a mean primary particle diameter of 23.14 ± 8.31 nm and a median diameter of 25.30 nm, with an observed range of 5.07–34.88 nm. The two most populated size intervals, 25–30 and 30–35 nm, contained a total of 53 particles, corresponding to 47.3% of the analyzed population (Figure 4B). The TEM-derived size distribution therefore confirmed that the analyzed particles were predominantly below 35 nm. These dimensions were consistent with the characteristic surface plasmon resonance region observed by UV–Vis spectroscopy.

The colloidal behavior of the synthesized AgNPs in aqueous dispersion was further evaluated by dynamic light scattering. The mean hydrodynamic radius (r_h) was 15.47 nm, corresponding to an equivalent hydrodynamic diameter of approximately 30.94 nm. The hydrodynamic dimensions were therefore of the same general size order as the TEM-derived primary particle dimensions.

TEM and DLS characterize different physical dimensions of the nanoparticle system and should therefore not be interpreted as directly equivalent. TEM measures the dimensions of individual particle cores in the dried state, whereas DLS estimates the hydrodynamic dimensions of particles dispersed in the liquid phase and includes contributions from the surrounding solvation layer and surface-associated species. Nevertheless, the TEM-derived particle sizes and the DLS-derived hydrodynamic diameter were of the same general order of magnitude.



(**A**)



(**B**)

Figure 4. Morphology and primary particle-size distribution of AgNPs synthesized by the glucose–citrate method. (**A**) Representative TEM micrograph; scale bar = 100 nm. (**B**) TEM-derived particle-size distribution based on measurements of 112 individual particles. The mean particle diameter was 23.14 ± 8.31 nm, the median diameter was 25.30 nm, and the observed range was 5.07–34.88 nm.

The mean zeta potential of the AgNP dispersion was −38.80 ± 0.63 mV (n = 5). The pronounced negative surface charge is consistent with substantial electrostatic stabilization of the colloidal dispersion and is compatible with the presence of citrate species at the nanoparticle interface. The magnitude of the measured zeta potential indicates strong

electrostatic repulsion between dispersed particles under the measurement conditions, which may contribute to limiting aggregation.

Overall, the combined TEM, DLS, and zeta-potential measurements demonstrated the formation of nanoscale AgNPs with TEM-derived primary particle diameters ranging from 5.07 to 34.88 nm and a negatively charged colloidal dispersion. These physicochemical characteristics provided the basis for subsequent evaluation of the AgNP-containing antibacterial formulations.

3.3. Antibacterial Activity of AgNP-Containing Formulations Against Escherichia coli

The antibacterial activity of the developed multicomponent formulations was evaluated against *Escherichia coli* using the presence or complete absence of visible bacterial growth after incubation as the experimental endpoint. The assay was performed with a relatively high initial bacterial load of approximately 7.5×10^6 CFU per assay. In all control plates, intensive confluent bacterial growth was observed, confirming the viability of the inoculum under the experimental conditions.

Initial screening demonstrated clear differences in antibacterial performance among the tested formulation variants (Table 1). Lactic acid alone, tested at concentrations of 0.25–2% in the corresponding stock component, did not prevent visible bacterial growth. Similarly, chitosan–lactic acid solutions without AgNPs and collagen did not produce complete growth suppression within the tested concentration range. Formulations containing lactic acid, AgNPs, and collagen but lacking chitosan also showed visible bacterial growth, even when the nominal Ag concentration in the prepared formulation was approximately 52 mg/L.

Table 1. Effect of Different Formulation Combinations and Concentrations on Visible Growth of *Escherichia coli.*

Variant	Lactic Acid (% *w*/*w*)	Chitosan:Lactic acid (% *w*/*w*)	Ag in Final Assay (µg/mL)	NaCl Fraction (*v*/*v*)	Collagen (% *w*/*w*)	*E. coli* Growth
Group A. Lactic acid + 0.9% NaCl (1:2, *v*/*v*)						
A1	2	—	—	2/3	—	+
A2	1	—	—	2/3	—	+
A3	0.5	—	—	2/3	—	+
A4	0.25	—	—	2/3	—	+
Group B. Chitosan–lactic acid component + 0.9% NaCl (1:2, *v*/*v*)						
B1	—	1:2	—	2/3	—	+
B2	—	0.5:1	—	2/3	—	+
B3	—	0.25:0.5	—	2/3	—	+
B4	—	0.125:0.25	—	2/3	—	+
Group C. Lactic acid + AgNP dispersion + collagen (1:1:1, *v*/*v*/*v*)						
C1	2	—	26	—	10	+
C2	1	—	26	—	10	+
C3	0.5	—	26	—	10	+
C4	0.25	—	26	—	10	+

Table 1. *Cont.*

Variant	Lactic Acid (% *w*/*w*)	Chitosan:Lactic acid (% *w*/*w*)	Ag in Final Assay (μg/mL)	NaCl Fraction (*v*/*v*)	Collagen (% *w*/*w*)	*E. coli* Growth
Group D. Chitosan–lactic acid + AgNP dispersion + collagen (1:1:1, *v*/*v*/*v*)						
D1	—	1:2	26	—	30	–
D2	—	0.5:1	26	—	15	–
D3	—	0.25:0.5	26	—	10	–
D4	—	0.125:0.25	26	—	5	–
Group E. Complete formulation with decreasing Ag concentration						
E1	—	1:2	26	—	10	–
E2	—	1:2	13	—	10	–
E3	—	1:2	6.5	—	10	–
E4	—	1:2	3.25	—	10	–
Group F. Complete formulation with simultaneous reduction in chitosan–lactic acid and Ag concentration						
F1	—	1:2	26	—	10	–
F2	—	0.5:1	13	—	10	–
F3	—	0.25:0.5	6.5	—	10	–
F4	—	0.125:0.25	3.25	—	10	–

Note: +, visible bacterial growth; −, complete absence of visible bacterial growth after incubation; —, component absent or not applicable. Lactic acid, chitosan, and collagen concentrations are expressed as % (*w*/*w*) in the separately prepared components before formulation mixing. For Groups C–F, the formulation components were mixed at 1:1:1 (*v*/*v*/*v*). For Groups A and B, one volume of the indicated component was mixed with two volumes of 0.9% NaCl (1:2, *v*/*v*). The Ag values shown in the table represent the calculated nominal concentration in the final 400 μL antibacterial assay mixture. Corresponding nominal concentrations in the AgNP dispersion of 157, 79, 39, and 20 mg/L were equivalent to approximately 52, 26, 13, and 6.5 mg/L in the prepared formulation and 26, 13, 6.5, and 3.25 μg/mL, respectively, in the final assay mixture.

In contrast, complete formulations containing the AgNP dispersion, chitosan in lactic acid, and collagen at a 1:1:1 (*v*/*v*/*v*) ratio completely suppressed visible *E. coli* growth under the assay conditions. This effect was maintained across several concentrations of the biopolymer components. For example, complete suppression was observed when the chitosan–lactic acid stock component was reduced from 1:2% to 0.125:0.25% and the collagen stock concentration was reduced from 30% to 5%, while the nominal Ag concentration in the prepared formulation was maintained at approximately 52 mg/L.

The effect of reducing the AgNP content of the complete formulation was subsequently examined. Serial two-fold dilution of the original AgNP dispersion decreased the nominal Ag concentration in the AgNP component from 157 to 79, 39, and 20 mg/L, corresponding to approximately 52, 26, 13, and 6.5 mg/L, respectively, in the prepared 1:1:1 formulation. Complete absence of visible *E. coli* growth was observed at all four concentrations. Thus, 6.5 mg/L was the lowest nominal Ag concentration evaluated in the prepared complete formulation that produced complete suppression of visible bacterial growth; after mixing with the bacterial inoculum and nutrient broth, this corresponded to approximately 3.25 μg/mL Ag in the final assay mixture. In comparison, the formulation containing lactic acid, Ag-

NPs, and collagen but no chitosan still showed visible growth at approximately 52 mg/L Ag in the prepared formulation, corresponding to approximately 26 µg/mL in the assay mixture. Therefore, complete growth suppression by the full formulation was retained at an eightfold lower Ag concentration than that used in this chitosan-free comparator.

The experiment was conducted twice independently, with three Petri dishes used for each treatment and control in each experiment. The absence of visible growth in the effective complete formulations was reproducible across all replicate plates. Representative plates showing complete growth suppression by the full formulation, growth in an incomplete formulation, and confluent growth in the untreated control are presented in Figure 5.

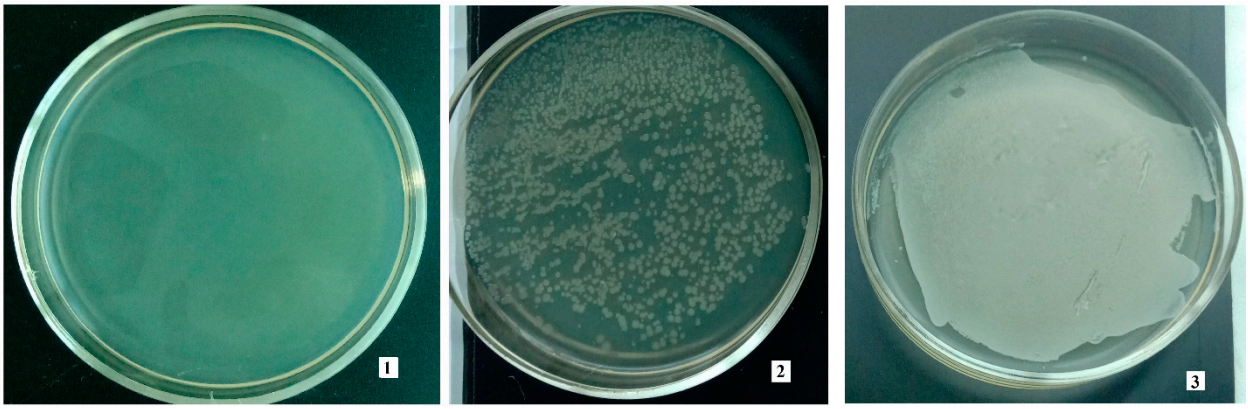


Figure 5. Representative *E. coli* growth patterns observed in the antibacterial assay: (1) complete absence of visible growth after treatment with formulation variant D4 (AgNP–chitosan–lactic acid–collagen); (2) visible bacterial growth after treatment with formulation variant C1 (lactic acid–AgNP–collagen); and (3) confluent bacterial growth in the untreated control.

These findings demonstrate that the AgNP–chitosan–lactic acid–collagen formulation was substantially more effective than the other tested component combinations. The consistently stronger antibacterial effect indicates that the combined action of AgNPs, chitosan, lactic acid, and collagen enhanced the overall antimicrobial performance of the system.

3.4. Preliminary In Vitro Assessment of the Concentration-Dependent Effect of AgNPs on Bovine Sperm Viability

A preliminary in vitro assay was conducted to evaluate the concentration-dependent effect of the synthesized AgNP dispersion on bovine sperm viability. Spermatozoa were exposed to nominal Ag concentrations ranging from 0.136 to 27.4 mg/L for 2 h, after which the proportion of viable cells was determined by eosin staining. The results are presented in Figure 6.

The mean proportion of viable spermatozoa in the untreated control was 71.26%. At the two lowest Ag concentrations, 0.136 and 0.274 mg/L, sperm viability was 68.53% and 66.46%, respectively. Although these values were lower than those of the control, neither treatment differed significantly from the control according to the multiple-comparison grouping shown in Figure 6 ($p > 0.05$).

A progressive decline in sperm viability was observed with increasing AgNP concentration. At 1.37 mg/L, mean viability decreased to 62.63%, representing a 12.1% reduction relative to the control and the first statistically significant decrease under the conditions of the assay. At 2.74 and 4.567 mg/L, viability decreased further to 53.63% and 45.77%, corresponding to reductions of approximately 24.7% and 35.8%, respectively.

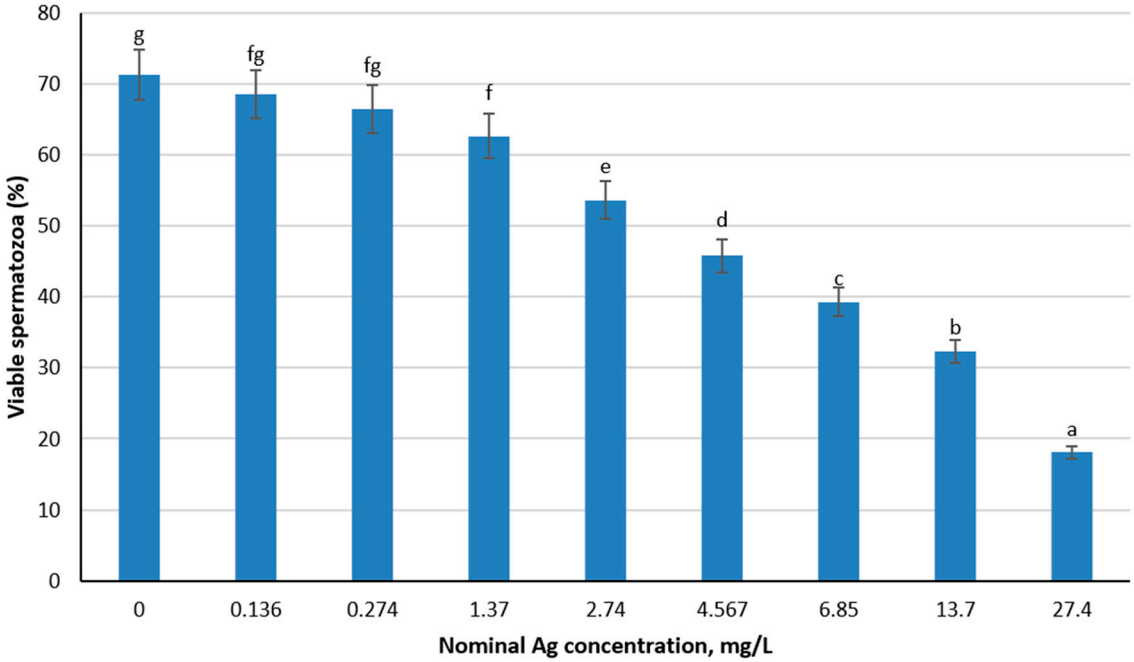


Figure 6. Effect of nominal Ag concentration in the AgNP dispersion on bovine sperm viability after 2 h of exposure. Data are presented as mean ± SD (n = 7 independent semen samples per group). Different lowercase letters indicate significant differences among groups at $p < 0.05$.

Further increases in nominal Ag concentration produced progressively greater effects. At 6.85 and 13.7 mg/L, sperm viability decreased to 39.31% and 32.32%, respectively. The strongest response was observed at 27.4 mg/L, where mean viability declined to 18.12%, representing a 74.6% reduction relative to the untreated control.

Overall, the AgNP dispersion produced a clear concentration-dependent reduction in bovine sperm viability after 2 h of exposure. Concentrations of 0.136 and 0.274 mg/L caused only limited changes relative to the untreated control, whereas statistically significant and progressively greater reductions were observed from 1.37 mg/L onward.

These results should be interpreted as a preliminary in vitro sperm viability assessment rather than a definitive toxicological assessment. The bovine sperm assay provides an initial indication of the concentration-dependent effect of the synthesized AgNP dispersion on bovine sperm viability but does not establish a safe exposure threshold for food-related applications. Further studies using standardized mammalian cell models, validated cytotoxicity assays, and additional endpoints are required to characterize the toxicological profile of the synthesized AgNPs more comprehensively.

4. Discussion

This study evaluated a modified glucose–citrate route for AgNP synthesis and examined the resulting nanoparticles within a multicomponent AgNP–chitosan–lactic acid–collagen formulation. The synthesized AgNPs exhibited nanoscale dimensions and a pronounced negative surface charge. The complete formulation suppressed visible *Escherichia coli* growth under the applied assay conditions, including at reduced silver concentrations, whereas the tested incomplete formulations did not achieve complete suppression. The AgNP dispersion also produced a concentration-dependent reduction in bovine sperm viability, emphasizing the need to consider antibacterial performance together with subsequent safety assessment.

The modified glucose–citrate route produced colloidal AgNP dispersions under relatively mild aqueous conditions. SPR maxima between 411.3 and 420.6 nm were observed

across the preliminary synthesis variants, while an earlier repeat synthesis using 35 mg of sodium citrate, measured separately with the KFK-3-01-ZOMZ spectrophotometer, showed a maximum at approximately 422 nm. Absorption in this region is characteristic of dispersed AgNPs, although UV–Vis spectroscopy alone cannot establish particle size or morphology [35]. The shifts in SPR position and intensity observed after changes in citrate content and reaction-temperature control are consistent with the sensitivity of citrate-mediated AgNP synthesis to reagent ratio, temperature, reaction time, pH, and precursor concentration [36,37]. Similar effects of citrate concentration and reaction conditions on AgNP growth and morphology have been reported previously [36,37]. These synthesis factors affect silver-ion reduction, nucleation, particle growth, and stabilization, supporting the need for controlled reaction conditions when reproducible colloidal systems are required. The optical data were therefore interpreted together with TEM and light-scattering measurements rather than as independent proof of particle size.

TEM confirmed nanoscale particle formation. Quantitative analysis of 112 particles yielded a mean primary diameter of 23.14 ± 8.31 nm, a median of 25.30 nm, and an observed range of 5.07–34.88 nm. Predominantly quasi-spherical particles were observed together with occasional irregular and anisotropic morphologies, which are consistent with the morphological heterogeneity reported for citrate-mediated AgNP synthesis [35–37]. DLS gave a mean hydrodynamic radius of 15.47 nm, corresponding to an equivalent hydrodynamic diameter of approximately 30.94 nm. Although TEM and DLS should not be interpreted as directly equivalent because they measure dried primary-particle dimensions and hydrodynamic dimensions in liquid, respectively; DLS also reflects the associated solvation layer and surface-bound species [38,39], both measurements placed the particles within the same general nanoscale size range. The zeta potential of −38.80 ± 0.63 mV was consistent with pronounced electrostatic stabilization under the measurement conditions. This negative surface charge is compatible with citrate-associated stabilization: negatively charged surface groups increase electrostatic repulsion between particles [40], and its magnitude is comparable with values reported for stable AgNP dispersions [24,41]. Das Neves et al. reported −36.4 mV before incorporation into biodegradable films [24]. High absolute zeta-potential values are generally associated with increased resistance to aggregation in electrostatically stabilized colloids [41]. However, the zeta-potential measurement should not be interpreted as direct evidence of long-term storage stability.

The principal antibacterial finding was that the complete AgNP–chitosan–lactic acid–collagen formulation suppressed visible *E. coli* growth, whereas the tested individual or incomplete component combinations did not achieve complete suppression. Lactic acid alone and chitosan combined with lactic acid allowed visible growth at the tested concentrations. Most importantly, complete suppression was retained at 6.5 mg/L nominal Ag in the prepared formulation, corresponding to approximately 3.25 μg/mL in the final 400 μL assay mixture. In contrast, the chitosan-free lactic acid–AgNP–collagen formulation still showed visible growth at approximately 52 mg/L Ag in the prepared formulation (approximately 26 μg/mL in the assay mixture). Thus, the observed antibacterial performance cannot be attributed solely to nominal silver concentration. Collagen served primarily as a viscous biopolymer carrier, whereas lactic acid enabled chitosan solubilization and may also contribute antimicrobial activity. However, the experimental design does not establish formal synergism or quantify the individual contribution of collagen and lactic acid; Ag release was not measured, and enhanced physicochemical stability of AgNPs within the complete formulation was not quantitatively demonstrated.

The present system also differs from previously reported AgNP–chitosan materials in formulation composition and experimental design. Ogungbesan et al. [23] generated AgNPs within an acetic-acid-based chitosan film, whereas the present study incorporated

separately synthesized citrate-stabilized AgNPs into a collagen–chitosan–lactic acid formulation. Das Neves et al. [24] studied biogenic AgNPs in starch/PBAT biodegradable films and additionally evaluated silver migration into chicken meat. In the present study, formulation components were systematically varied while maintaining comparable volumetric proportions, with omitted components replaced by equivalent volumes of 0.9% NaCl. This matched-component design, together with maintenance of antibacterial activity at reduced Ag concentrations, distinguishes the present formulation from the simple addition of AgNPs to an established chitosan matrix.

Previous studies confirm that incorporation of AgNPs into chitosan-containing matrices can substantially influence antibacterial performance. Wei et al. [42] reported MIC and MBC values of 10 μg/mL against *E. coli* for chitosan-based AgNPs, compared with an MIC of 48 μg/mL for chitosan alone. Yoksan and Chirachanchai [43] reported an MIC of 5.64 μg/mL against *E. coli*, *Staphylococcus aureus*, and *Bacillus cereus* for 20–25 nm AgNPs dispersed in irradiated chitosan, while Behera et al. [44] reported an *E. coli* MIC of 1.56 μg/mL for a AgNP–chitosan nanocomposite and an additive interaction (FIC = 0.73). In that study, the MICs for AgNPs alone and chitosan alone were 6.25 and 3.125 μg/mL, respectively, reinforcing the need to distinguish improved formulation performance from formal synergism. Tankhiwale and Bajpai [45] likewise observed almost complete suppression of *E. coli* using AgNP-loaded chitosan-lactate films compared with the corresponding chitosan matrix, providing a particularly relevant precedent for combining silver with a chitosan–lactate system. Collectively, these studies demonstrate that antibacterial performance depends strongly on nanoparticle characteristics, matrix composition, and the experimental assay.

Other biopolymer systems further illustrate the importance of matrix and exposure conditions. López-Carballo et al. [46] showed that the antibacterial activity of AgNP-containing chitosan films against *E. coli* increased substantially in the diluted growth medium, demonstrating the influence of the surrounding matrix. At 0.1% silver, these films produced an approximately 0.9-log reduction in *E. coli* in Mueller–Hinton broth, with greater reductions at higher silver contents; dilution of the medium increased reductions to approximately 3 log cycles. Li et al. [47] reported antibacterial rates exceeding 99% for AgNP-loaded collagen–chitosan dressings, whereas Yang et al. [48] demonstrated antibacterial activity and strawberry-preservation potential for AgNP-loaded chitosan/PVA films. The collagen–chitosan dressings were effective against *S. aureus*, *E. coli*, and *Pseudomonas aeruginosa* at loadings above 0.3 mg/cm^2 AgNPs. Although this biomedical system differs from the present food-related formulation, it supports the feasibility of collagen–chitosan matrices as antimicrobial carriers. Yang et al. reported an *E. coli* inhibition zone of 16.07 mm at 0.019% (*w*/*w*) AgNPs, with reduced strawberry deterioration during storage; the material format and assay differed from those used here. In the present study, the lowest tested effective concentration corresponded to approximately 3.25 μg/mL Ag in the final assay mixture, which is obtained by mixing 200 μL of formulation with 200 μL of inoculum–broth phase. This exposure lies within the same general concentration range as several reported MIC values. However, this comparison is only contextual: the present endpoint was obtained using a qualitative direct-contact plating assay rather than standardized broth microdilution, and 3.25 μg/mL must therefore not be interpreted as an MIC.

The direct-contact assay used a relatively high bacterial challenge of approximately 7.5×10^6 CFU per assay. Complete absence of visible growth was reproducible across the effective full-formulation replicates, whereas the controls showed confluent growth. Nevertheless, this qualitative endpoint is not equivalent to a standardized MIC or MBC determination. This reproducibility across independent experiments strengthens the evidence for an antibacterial effect under the tested conditions, while the qualitative readout

limits the conclusions that can be drawn about its magnitude. The results therefore support antibacterial activity under the applied conditions but require confirmation using standardized quantitative assays and a broader panel of foodborne microorganisms.

Because formulation-only blank plates without bacterial inoculation were not included, possible visual interference from formulation opacity or surface-layer formation could not be excluded independently. Although bacterial colonies were morphologically distinguishable from the relatively uniform formulation-associated turbidity and no delayed growth was observed during extended monitoring, future studies should include dedicated matrix blanks together with quantitative colony-counting or standardized susceptibility methods.

The preliminary bovine sperm assay showed a concentration-dependent reduction in viability following exposure to the AgNP dispersion alone. Viability at 0.136 and 0.274 mg/L remained statistically comparable with the untreated control, whereas the first significant reduction occurred at 1.37 mg/L and viability declined further with increasing concentration, reaching 18.12% at 27.4 mg/L. This pattern is consistent with the concentration-dependent biological effects of AgNPs reported in the literature, which are influenced by particle size, surface chemistry, aggregation state, exposure duration, and Ag^+ release [35,41]. Importantly, the sperm assay did not evaluate the complete AgNP–chitosan–lactic acid–collagen formulation and therefore cannot demonstrate an improved antibacterial–biological safety balance for the multicomponent system. Spermatozoa are sensitive to oxidative stress, membrane damage, and disturbances in mitochondrial function, supporting their use as a preliminary screening model. Nevertheless, the antibacterial and sperm experiments involved different biological systems and exposure conditions. Moreover, bovine sperm viability is only a preliminary biological screening endpoint and cannot establish food-contact safety, a regulatory safe concentration, or a direct therapeutic or safety window. Further standardized toxicological evaluation is therefore required.

The potential use of AgNP-containing formulations in food-contact applications also requires careful consideration of silver migration. Das Neves et al. [24] demonstrated that AgNP-containing biodegradable films had antibacterial activity against *Salmonella* but also reported substantial silver migration into chicken meat, illustrating that antibacterial efficacy does not itself establish food-contact safety. Reviews similarly identify migration, bioaccumulation, cytotoxicity, and regulatory uncertainty as important barriers to broader application of AgNP-based food-packaging systems [15,49]. The antimicrobial contribution of chitosan is also influenced by factors such as molecular weight, degree of deacetylation, pH, and formulation conditions [50,51], while reviews of AgNP-containing polymeric and biopolymer-based food-packaging systems further emphasize the importance of matrix composition, silver release, migration, and safety assessment [52,53]. The present formulation should therefore be regarded as an experimental antimicrobial system rather than a ready-to-use food preservative. Although complete visible-growth suppression was retained at 6.5 mg/L Ag in the prepared formulation, corresponding to approximately 3.25 μg/mL in the final assay mixture, future work should include standardized mammalian-cell cytotoxicity testing, determination of Ag^+ and total silver release, migration studies in actual food matrices, quantitative antimicrobial testing against additional foodborne microorganisms, and validation in meat or poultry systems under refrigerated storage conditions.

5. Conclusions

Silver nanoparticles synthesized by the modified glucose–citrate method exhibited nanoscale dimensions and a pronounced negative surface charge consistent with electrostatic stabilization of the colloidal dispersion. When incorporated into the complete AgNP–chitosan–lactic acid–collagen formulation, the nanoparticles produced marked an-

tibacterial activity against *Escherichia coli*. Complete absence of visible bacterial growth was observed at all tested concentrations of the complete formulation, including the lowest evaluated nominal Ag concentration of 6.5 mg/L in the prepared formulation, corresponding to approximately 3.25 μg/mL in the final antibacterial assay mixture, whereas the other tested formulation variants did not achieve complete growth suppression. The preliminary bovine sperm assay showed a concentration-dependent decrease in cell viability following exposure to the AgNP dispersion alone, with statistically significant effects observed from 1.37 mg/L onward. These findings indicate that the antibacterial performance of AgNP-based formulations should be considered together with the concentration-dependent effects of AgNP exposure on bovine sperm viability. Overall, the results support the further development of the AgNP–chitosan–lactic acid–collagen system as a potential antimicrobial formulation for food-related applications. Further studies should include standardized quantitative antimicrobial assays, mammalian-cell cytotoxicity testing, silver-ion and total-silver release measurements, migration studies, and validation in real food matrices under relevant storage conditions.

6. Patents

Suychinov, A.; Derbyshev, K.; Yessimbekov, Z.; Asserzhanov, D. Method for Producing Silver Nanoparticles. Utility Model Patent of the Republic of Kazakhstan No. 12248, published 22 May 2026, Bulletin No. 20.

Author Contributions: Conceptualization, D.A. and E.O.; Data curation, Z.Y.; Investigation, K.D. and D.A.; Methodology, K.D., Z.Y., D.A. and E.O.; Project administration, A.S.; Software, D.A.; Supervision, A.S.; Validation, A.S.; Visualization, K.D. and Z.Y.; Writing—original draft, K.D. and E.O.; Writing—review & editing, A.S., Z.Y. and E.O. All authors have read and agreed to the published version of the manuscript.

Funding: This research was funded by the Ministry of Science and Higher Education of the Republic of Kazakhstan under Grant No. BR24992938.

Institutional Review Board Statement: The study was conducted in accordance with the Declaration of Helsinki and approved by the Local Ethics Committee of the Institutional Review Board of Shakarim University, Semey, Kazakhstan (Protocol No. 9.2, approved on 20 May 2026).

Informed Consent Statement: Not applicable.

Data Availability Statement: The original contributions presented in this study are included in the article. Further inquiries can be directed to the corresponding author.

Conflicts of Interest: The authors declare no conflicts of interest.

References

1. Khalid, T.; Hdaifeh, A.; Federighi, M.; Cummins, E.; Boué, G.; Guillou, S.; Tesson, V. Review of Quantitative Microbial Risk Assessment in Poultry Meat: The Central Position of Consumer Behavior. *Foods* **2020**, *9*, 1661. [CrossRef] [PubMed]
2. Salama, Y.; Chennaoui, M. Understanding Microbial Contamination in Meat and Poultry Production. *J. Res. Agric. Food Sci.* **2024**, *1*, 87–107. [CrossRef]
3. Chowdhury, M.A.H.; Ashrafudoulla, M.; Mevo, S.I.U.; Mizan, M.F.R.; Park, S.H.; Ha, S.D. Current and Future Interventions for Improving Poultry Health and Poultry Food Safety and Security: A Comprehensive Review. *Compr. Rev. Food Sci. Food Saf.* **2023**, *22*, 1555–1596. [CrossRef] [PubMed]
4. Moura-Alves, M.; Esteves, A.; Ciríaco, M.; Silva, J.A.; Saraiva, C. Antimicrobial and Antioxidant Edible Films and Coatings in the Shelf-Life Improvement of Chicken Meat. *Foods* **2023**, *12*, 2308. [CrossRef] [PubMed]
5. Chavan, P.; Vashishth, R. Antimicrobial Resistance in Foodborne Pathogens: Consequences for Public Health and Future Approaches. *Discov. Appl. Sci.* **2025**, *7*, 623. [CrossRef]

6. Dushayeva, L.Z. Antimicrobial Resistance in Foodborne *Escherichia coli* and Salmonella spp. from Animal-Origin Foods: Transmission Pathways, Global Surveillance Gaps, and Alternative Therapeutic Strategies. *Vet. World* **2025**, *18*, 3288–3305. [CrossRef] [PubMed]
7. Abdullah, A.Y.; Al-Nabulsi, A.; Jamama'h, M.; Khataybeh, B.; Al-Ghadi, M. Microbial Shelf Life and Quality Assessment of Broiler Breast Meat: The Role of Cold Storage and Carcass Weight. *Foods* **2025**, *14*, 640. [CrossRef] [PubMed]
8. Marmion, M.; Macori, G.; Ferone, M.; Whyte, P.; Scannell, A.G.M. Survive and Thrive: Control Mechanisms That Facilitate Bacterial Adaptation to Survive Manufacturing-Related Stress. *Int. J. Food Microbiol.* **2022**, *368*, 109612. [CrossRef] [PubMed]
9. Pérez, E.; Sanjuán, E.; Jůzl, M.; Raposo, A.; Saraiva, A.; Jaber, J.R.; Carrascosa, C. Active Antimicrobial Packaging Systems: Mechanisms of Microbial Control and Applications in Food Preservation. *Biology* **2026**, *15*, 325. [CrossRef] [PubMed]
10. Menichetti, A.; Mavridi-Printezi, A.; Mordini, D.; Montalti, M. Effect of Size, Shape and Surface Functionalization on the Antibacterial Activity of Silver Nanoparticles. *J. Funct. Biomater.* **2023**, *14*, 244. [CrossRef] [PubMed]
11. Dakal, T.C.; Kumar, A.; Majumdar, R.S.; Yadav, V. Mechanistic Basis of Antimicrobial Actions of Silver Nanoparticles. *Front. Microbiol.* **2016**, *7*, 1831. [CrossRef] [PubMed]
12. Holubnycha, V.; Husak, Y.; Korniienko, V.; Bolshanina, S.; Tveresovska, O.; Myronov, P.; Holubnycha, M.; Butsyk, A.; Borén, T.; Banasiuk, R.; et al. Antimicrobial Activity of Two Different Types of Silver Nanoparticles against a Wide Range of Pathogenic Bacteria. *Nanomaterials* **2024**, *14*, 137. [CrossRef] [PubMed]
13. Sánchez-López, E.; Gomes, D.; Esteruelas, G.; Bonilla, L.; Lopez-Machado, A.L.; Galindo, R.; Cano, A.; Espina, M.; Ettcheto, M.; Camins, A.; et al. Metal-Based Nanoparticles as Antimicrobial Agents: An Overview. *Nanomaterials* **2020**, *10*, 292. [CrossRef] [PubMed]
14. Rabiee, N.; Ahmadi, S.; Akhavan, O.; Luque, R. Silver and Gold Nanoparticles for Antimicrobial Purposes against Multi-Drug Resistance Bacteria. *Materials* **2022**, *15*, 1799. Correction in *Materials* **2024**, *17*, 2841. [CrossRef] [PubMed]
15. Jangid, H.; Joshi, H.C.; Dutta, J.; Ahmad, A.; Alshammari, M.B.; Hossain, K.; Pant, G.; Kumar, G. Advancing Food Safety with Biogenic Silver Nanoparticles: Addressing Antimicrobial Resistance, Sustainability, and Commercial Viability. *Food Chem. X* **2025**, *26*, 102298. [CrossRef] [PubMed]
16. Carrión, M.G.; Corripio, M.A.R.; Hidalgo Contreras, J.V.; Rangel Marrón, M.; Morales Olán, G.; Hernández Cázares, A.S. Optimization and Characterization of Taro Starch, Nisin, and Sodium Alginate-Based Biodegradable Films: Antimicrobial Effect in Chicken Meat. *Poult. Sci.* **2023**, *102*, 103100. [CrossRef] [PubMed]
17. Eker, F.; Akdaşçi, E.; Duman, H.; Bechelany, M.; Karav, S. Green Synthesis of Silver Nanoparticles Using Plant Extracts: A Comprehensive Review of Physicochemical Properties and Multifunctional Applications. *Int. J. Mol. Sci.* **2025**, *26*, 6222. [CrossRef] [PubMed]
18. Olaifa, O.P.; Bolaji, O.B.; Adedeji, A.S.; Onihunwa, J.O.; Sulyman, S.; Adetona, A. Effects of Silver Nanoparticles on Meat Preservation. *Ethiop. J. Environ. Stud. Manag.* **2020**, *13*, 731–738.
19. Park, K.; Lee, Y. The Stability of Citrate-Capped Silver Nanoparticles in Isotonic Glucose Solution for Intravenous Injection. *J. Toxicol. Environ. Health A* **2013**, *76*, 1236–1245. [CrossRef] [PubMed]
20. Noga, M.; Milan, J.; Frydrych, A.; Jurowski, K. Toxicological Aspects, Safety Assessment, and Green Toxicology of Silver Nanoparticles (AgNPs)—Critical Review: State of the Art. *Int. J. Mol. Sci.* **2023**, *24*, 5133. [CrossRef] [PubMed]
21. Muñoz-Tebar, N.; Pérez-Álvarez, J.A.; Fernández-López, J.; Viuda-Martos, M. Chitosan Edible Films and Coatings with Added Bioactive Compounds: Antibacterial and Antioxidant Properties and Their Application to Food Products: A Review. *Polymers* **2023**, *15*, 396. [CrossRef] [PubMed]
22. Ezati, P.; Khan, A.; Bhattacharya, T.; Zaitoon, A.; Zhang, W.; Roy, S.; Rhim, J.-W.; Lim, L.-T. Recent Advances in Collagen and Collagen-Based Packaging Materials: A Review. *ACS Food Sci. Technol.* **2025**, *5*, 1767–1784. [CrossRef]
23. Ogungbesan, S.O.; Buxaderas, E.; Adedokun, R.A.; Moglie, Y.; Grijalvo, S.; García, M.T.; Bingbing, C.; Díaz Díaz, D.; Fu, G. Synthesis and Characterization of Chitosan–Silver Nanocomposite Film: Antibacterial and Cytotoxicity Study. *ChemistrySelect* **2024**, *9*, e202404909. [CrossRef]
24. das Neves, M.d.S.; Scandorieiro, S.; Pereira, G.N.; Ribeiro, J.M.; Seabra, A.B.; Dias, A.P.; Yamashita, F.; Martinez, C.B.d.R.; Kobayashi, R.K.T.; Nakazato, G. Antibacterial Activity of Biodegradable Films Incorporated with Biologically Synthesized Silver Nanoparticles and the Evaluation of Their Migration to Chicken Meat. *Antibiotics* **2023**, *12*, 178. [CrossRef] [PubMed]
25. Bogacheva, N.V.; Tarbeeva, K.A.; Ogorodova, N.Y.; Khasanshina, Z.R.; Chernyadyev, A.V.; Tuneva, N.A. Method for Producing Silver Nanoparticles with a Size of 30 ± 3 nm. Russian Federation Patent RU2729991C1, 13 August 2020.
26. Cooke, J.; Hebert, D.; Kelly, J.A. Sweet Nanochemistry: A Fast, Reliable Alternative Synthesis of Yellow Colloidal Silver Nanoparticles Using Benign Reagents. *J. Chem. Educ.* **2015**, *92*, 345–349. [CrossRef]
27. Ndikau, M.; Noah, N.M.; Andala, D.M.; Masika, E. Green Synthesis and Characterization of Silver Nanoparticles Using *Citrullus lanatus* Fruit Rind Extract. *Int. J. Anal. Chem.* **2017**, *2017*, 8108504. [CrossRef] [PubMed]

28. Ebrahiminezhad, A.; Berenjian, A.; Ghasemi, Y. Template-Free Synthesis of Natural Carbohydrate-Functionalized Fluorescent Silver Nanoclusters. *IET Nanobiotechnol.* **2016**, *10*, 120–123. [CrossRef] [PubMed]
29. Stetefeld, J.; McKenna, S.A.; Patel, T.R. Dynamic Light Scattering: A Practical Guide and Applications in Biomedical Sciences. *Biophys. Rev.* **2016**, *8*, 409–427. [CrossRef]
30. Anton Paar GmbH. Litesizer 100/500 Reference Guide. Available online: https://wiki.anton-paar.com/en/zeta-potential/ (accessed on 28 August 2026).
31. Talebpour, C.; Fani, F.; Ouellette, M.; Fairfax, M.; Alamdari, H.; Salimnia, H. Identification and mitigation of blood's interference with the antimicrobial activity of $AgNbO_3$ particles. *PLoS ONE* **2025**, *20*, e0313055. [CrossRef] [PubMed]
32. Dias, S.D.D.F.; Pinto-de-Andrade, L.; Rolo, J.; Gaspar, C.; Gomes-Ruivo, P.; Oliveira, A.S.; Ferreira, S.S.; Palmeira-de-Oliveira, R.; Martinez-de-Oliveira, J.; Gonçalves, J.C.; et al. Reproductive Toxicity Assessment of Four Portuguese Plant Hydrolates: Effects on Oocyte Maturation and Sperm Viability. *Animals* **2025**, *15*, 2838. [CrossRef] [PubMed]
33. Lukáčová, J.; Jambor, T.; Lukáč, N. In Vitro Assessment of Exposure to Nonylphenol on Viability of Bovine Spermatozoa. *J. Microbiol. Biotechnol. Food Sci.* **2014**, *3*, 128–130.
34. Aksu, E.H.; Kurtuluş, E.Y.; Aktürk, B. The Effects of Different Thawing Procedures on Spermatological Parameters of Frozen Bull Sperm. *Turk. J. Agric. Food Sci. Technol.* **2024**, *12*, 1068–1071. [CrossRef]
35. Zhang, X.-F.; Liu, Z.-G.; Shen, W.; Gurunathan, S. Silver Nanoparticles: Synthesis, Characterization, Properties, Applications, and Therapeutic Approaches. *Int. J. Mol. Sci.* **2016**, *17*, 1534. [CrossRef] [PubMed]
36. Ranoszek-Soliwoda, K.; Tomaszewska, E.; Socha, E.; Krzyczmonik, P.; Ignaczak, A.; Orlowski, P.; Krzyzowska, M.; Celichowski, G.; Grobelny, J. The Role of Tannic Acid and Sodium Citrate in the Synthesis of Silver Nanoparticles. *J. Nanopart. Res.* **2017**, *19*, 273. [CrossRef] [PubMed]
37. La Spina, R.; Mehn, D.; Fumagalli, F.; Holland, M.; Reniero, F.; Rossi, F.; Gilliland, D. Synthesis of Citrate-Stabilized Silver Nanoparticles Modified by Thermal and pH-Preconditioned Tannic Acid. *Nanomaterials* **2020**, *10*, 2031. [CrossRef] [PubMed]
38. Bhattacharjee, S. DLS and Zeta Potential—What They Are and What They Are Not. *J. Control. Release* **2016**, *235*, 337–351. [CrossRef] [PubMed]
39. Vazquez-Muñoz, R.; Meza-Villezcas, A.; Fournier, P.G.J.; Soria-Castro, E.; Juarez-Moreno, K.; Gallego-Hernández, A.L.; Bogdanchikova, N.; Vazquez-Duhalt, R.; Huerta-Saquero, A. Enhancement of Antibiotic Antimicrobial Activity Due to the Silver Nanoparticle Impact on the Cell Membrane. *PLoS ONE* **2019**, *14*, e0224904. [CrossRef] [PubMed]
40. Lee, S.H.; Jun, B.-H. Silver Nanoparticles: Synthesis and Application for Nanomedicine. *Int. J. Mol. Sci.* **2019**, *20*, 865. [CrossRef] [PubMed]
41. Bruna, T.; Maldonado-Bravo, F.; Jara, P.; Caro, N. Silver Nanoparticles and Their Antibacterial Applications. *Int. J. Mol. Sci.* **2021**, *22*, 7202. [CrossRef] [PubMed]
42. Wei, D.; Sun, W.; Qian, W.; Ye, Y.; Ma, X. The synthesis of chitosan-based silver nanoparticles and their antibacterial activity. *Carbohydr. Res.* **2009**, *344*, 2375–2382. [CrossRef] [PubMed]
43. Yoksan, R.; Chirachanchai, S. Silver nanoparticle-loaded chitosan–starch based films: Fabrication and evaluation of tensile, barrier and antimicrobial properties. *Mater. Sci. Eng. C* **2010**, *30*, 891–897. [CrossRef]
44. Behera, S.S.; Majumdar, A.G.; Gullani, H.; Roy, A.L.; Dash, A.K.; Behera, P.K.; Parwez, Z.; Giri, S.; Mohanty, P.S.; Ray, L. Green synthesis of silver-chitosan nanocomposite exhibits promising antibiofilm properties against pathogenic bacteria *Escherichia coli* and *Staphylococcus aureus*. *The Microbe* **2025**, *6*, 100264. [CrossRef]
45. Tankhiwale, R.; Bajpai, S.K. Silver-Nanoparticle-Loaded Chitosan Lactate Films with Fair Antibacterial Properties. *J. Appl. Polym. Sci.* **2010**, *115*, 1894–1900. [CrossRef]
46. López-Carballo, G.; Higueras, L.; Gavara, R.; Hernández-Muñoz, P. Silver Ions Release from Antibacterial Chitosan Films Containing In Situ Generated Silver Nanoparticles. *J. Agric. Food Chem.* **2013**, *61*, 260–267. [CrossRef] [PubMed]
47. Li, R.; Xu, Z.; Jiang, Q.; Zheng, Y.; Chen, Z.; Chen, X. Characterization and biological evaluation of a novel silver nanoparticle-loaded collagen-chitosan dressing. *Regen. Biomater.* **2020**, *7*, 371–380. [CrossRef] [PubMed]
48. Yang, D.; Liu, Q.; Gao, Y.; Wan, S.; Meng, F.; Weng, W.; Zhang, Y. Characterization of silver nanoparticles loaded chitosan/polyvinyl alcohol antibacterial films for food packaging. *Food Hydrocoll.* **2023**, *136*, 108305. [CrossRef]
49. Okur, E.E.; Eker, F.; Akdaşçi, E.; Bechelany, M.; Karav, S. Comprehensive Review of Silver Nanoparticles in Food Packaging Applications. *Int. J. Mol. Sci.* **2025**, *26*, 9842. [CrossRef] [PubMed]
50. Nasaj, M.; Chehelgerdi, M.; Asghari, B.; Ahmadieh-Yazdi, A.; Asgari, M.; Kabiri-Samani, S.; Sharifi, E.; Arabestani, M. Factors Influencing the Antimicrobial Mechanism of Chitosan Action and Its Derivatives: A Review. *Int. J. Biol. Macromol.* **2024**, *277*, 134321. [CrossRef] [PubMed]
51. Kong, M.; Chen, X.G.; Xing, K.; Park, H.J. Antimicrobial Properties of Chitosan and Mode of Action: A State-of-the-Art Review. *Int. J. Food Microbiol.* **2010**, *144*, 51–63. [CrossRef] [PubMed]

52. Carbone, M.; Donia, D.T.; Sabbatella, G.; Antiochia, R. Silver Nanoparticles in Polymeric Matrices for Fresh Food Packaging. *J. King Saud. Univ. Sci.* **2016**, *28*, 273–279. [CrossRef]
53. Kraśniewska, K.; Galus, S.; Gniewosz, M. Biopolymer-Based Materials Containing Silver Nanoparticles as Active Packaging for Food Applications—A Review. *Int. J. Mol. Sci.* **2020**, *21*, 698. [CrossRef] [PubMed]

Disclaimer/Publisher's Note: The statements, opinions and data contained in all publications are solely those of the individual author(s) and contributor(s) and not of MDPI and/or the editor(s). MDPI and/or the editor(s) disclaim responsibility for any injury to people or property resulting from any ideas, methods, instructions or products referred to in the content.